

## HYBRID AL<sub>2</sub>O<sub>3</sub>-CU-WATER NANOFLUID-FLOW AND HEAT TRANSFER OVER VERTICAL DOUBLE FORWARD-FACING STEP

by

**Hussein TOGUN<sup>a\*</sup>, Raad Z. HOMOD<sup>b</sup>, and Tuqa ABDULRAZZAQ<sup>c</sup>**

<sup>a</sup> Department of Biomedical Engineering, University of Thi-Qar, Nassiriya, Iraq

<sup>b</sup> Department of Oil and Gas Engineering, Basra University for Oil and Gas, Basra, Iraq

<sup>c</sup> Department of Petroleum and Gas Engineering, University of Thi-Qar, Nassiriya, Iraq

Original scientific paper

<https://doi.org/10.2298/TSCI201130080T>

*Turbulent heat transfer and hybrid Al<sub>2</sub>O<sub>3</sub>-Cu-nanofluid over vertical double forward-facing-step is numerically conducted. The k-ε standard model based on finite volume method in 2-D are applied to investigate the influences of Reynolds number, step height, volume fractions hybrid Al<sub>2</sub>O<sub>3</sub>-Cu-nanofluid on thermal performance. In this paper, different step heights for three cases of vertical double forward-facing step are adopted by five different of volume fractions of hybrid (Al<sub>2</sub>O<sub>3</sub>-Cu-water) nanofluid varied for 0.1, 0.33, 0.75, 1, and 2, while the Reynolds number different between 10000 to 40000 with temperature is constant. The main findings revealed that rise in local heat transfer coefficients with raised Reynolds number and maximum heat transfer coefficient was noticed at Re = 40000. Also rises in heat transfer coefficient detected with increased volume concentrations of hybrid (Al<sub>2</sub>O<sub>3</sub>-Cu-water) nanofluid and the maximum heat transfer coefficient found at hybrid Al<sub>2</sub>O<sub>3</sub>-Cu-water nanofluid of 2% in compared with others. It is also found that rise in surface heat transfer coefficient at 1<sup>st</sup> step-Case 2 was greater than at 1<sup>st</sup> step-Case 1 and 3 while was higher at 2<sup>nd</sup> step-Case 3. Average heat transfer coefficient with Reynolds number for all cases are presented in this paper and found that the maximum average heat transfer coefficient was at Case 2 compared with Case 1 and 3. Gradually increases in skin friction coefficient remarked at 1<sup>st</sup> and 2<sup>nd</sup> steps of the channel and drop in skin friction coefficient was obtained with increased of Reynolds number. Counter of velocity was presented to show the re-circulation regions at 1<sup>st</sup> and 2<sup>nd</sup> steps as clarified the enrichment in heat transfer rate. Furthermore, the counter of turbulence kinetic energy contour was displayed to provide demonstration for achieving thermal performance at second step for all cases.*

Key words: hybrid nanofluids, augmentation heat transfer, forward-facing step, re-circulation flow

### Introduction

In previous years, many efforts were achieved to optimize thermal performance in different manufacturing applications. Flow over forward-facing step (FFS) is one of the important aims for enhancing efficiency of thermal performance. Scheit *et al.* [1] numerically studied turbulent flow over FFS by using direct numerical simulation (DNS) based on finite volume method. Their results showed that there is slightly collected streaklines due to re-circulation flow at step. Also Alibek and Yeldos [2] presented numerical investigation on influence geometry for

\* Corresponding author, e-mail: htokan\_2004@yahoo.com; hussein-tokan@utq.edu.iq

fluid-flow and heat transfer over Forward-Backward facing step by employing DNS. Turbulent water flow and heat transfer over horizontal DFFS step is numerically studied by Togun *et al.* [3]. Increasing of Reynolds number and step height was noticed lead to rise in Nusselt number. Biswas *et al.* [4] carried out on effect step height of BFS on feature of fluid-flow and found that due to rise in step height the separation length increase non-linearly and acceptable with Armaly *et al.* [5]. Study fluid-flow and heat transfer over horizontal DFFS reported by Oztop *et al.* [6]. Enrichment in heat transfer was detected by influence of aspect ratio,  $Ar$ , and highest augmentation was got at  $Ar = 1$ . Furthermore, influence of corrugated wall combined with BFS passage on heat transfer and fluid-flow were numerically studied by Hilo *et al.* [7]. The results revealed that the greatest heat transfer improvement was occurred with trapezoidal corrugation at 4 mm amplitude height and 20 mm pitch diameter and the improved the Nusselt number, was up to 62% at Reynolds number,  $Re = 5000$ .

Generally, effects of modification the channels on thermal performance such as reducing or expanding passage, fins, ribbed channel are investigated in various numerical and experimental studies [8-22].

In the new decades, considered efforts done to verification help using nanofluids in disparate applications [23-34]. Kherbeet *et al.* [35, 36] conducted experimental and numerical study on laminar nanofluids flow and heat transfer over microscale FFS. The maximum Nusselt number was found about 30.6% with 1% SiO<sub>2</sub> nanofluid. Using  $k-\epsilon$  model for study heat transfer and nanofluids flow over a horizontal single and double FFS is investigated by Togun *et al.* [37, 38]. The authors observed that increase in step height, volume fractions of nanofluids, and Reynolds number lead to rise in Nusselt number. While Safaei *et al.* [39] adopted shear stress transport  $k-\omega$  model to analysis turbulent (FMWCNT) nanofluids and heat transfer over a FFS. Increases in heat transfer factor was noticed with rise both of Reynolds number and volume fractions. Laminar nanofluid-flow and heat transfer over a BFS channel with an elastic bottom wall was numerically studied by Selimefendigil and Oztop [40]. They found that increases in average Nusselt number was about 30.65% with using nanoparticle and highest volume fraction for cylindrical particle shapes also obtain improvement in Nusselt number was about 50.58% and 33% by changing the elastic modulus of the hot wall and size of elastic part. Ahmed *et al.* [41] presented experimentally study of heat transfer and Al<sub>2</sub>O<sub>3</sub>-nanofluid-flow over horizontal BFS channel. The results found that increases in average heat transfer coefficient was 9.6% at Reynolds number of 4000 and 26.3% at Reynolds number of 16000 for concentration of 0.1%. The Al<sub>2</sub>O<sub>3</sub>-nanofluids.

Recently, researchers found new feature of nanofluids with higher thermal conductivity by mixture two or more kinds of different nanoparticles were namely hybrid nanofluids.

The earlier investigate on using hybrid was reported in study of Turcu *et al.* [42] by using multiwalled carbon nanotubes (MWCNT), Fe<sub>2</sub>O<sub>3</sub> nanoparticles and polypyrene-carbon nanotube (PPY-CNT). Jana *et al.* [43] discovered that thermal conductivity of (CNT-AuNP) and (CNT-CuNP) were decrease than those with single nanoparticles due to influences of nanoparticle compatibility. Saha [44], Hussein *et al.* [45], and Takabi and Salahi [46] presented investigation on laminar Al<sub>2</sub>O<sub>3</sub>-Cu-water hybrid nanofluid-flow and heat transfer in a wavy pipe by employing (FVM). They found that thermal performance for using hybrid nanofluids was higher than that by similar nanofluids. Mehrez and Cafsi [47] numerically studied of laminar Al<sub>2</sub>O<sub>3</sub>-Cu-water hybrid nanofluids flow and heat transfer over BFS by applying FVM. The authors obtained that improve in Nusselt number with increased volume concentrations of hybrid nanofluids and Reynolds number. Heat transfer and nanofluids (CuO and MgO) flow over a BFS were experimentally studied by Hilo *et al.* [48]. They obtained that the Nusselt

number was improved up to 11% at 0.05 volume fractions in compared to pure EG and found performance evaluation criteria at volume fractions of (CuO-EG nanofluid) and  $Re = 2000$  was greater than the MgO-EG nanofluid. Recently, Salman *et al.* [49] conducted a review on using hybrid nanofluid-flow and heat transfer over BFS and FFS and display the earlier researches on the augmentation in heat transfer for different geometries.

From the early studies, there are very limited researches done on hybrid nanofluid and heat transfer over BFS, furthermore study for hybrid nanofluid-flow over FFS has been not studied yet hence the goal of the current research is to analysis thermal characterization of hybrid nanofluid-flow over DFFS.

**Description of the physical problem**

The design which adopted in this model presented in fig. 1. The dimensions of the model supported on Abdulrazzaq *et al.* [50] by three different step heights change from 1-2 cm for 1<sup>st</sup> and 2<sup>nd</sup> steps as generated three cases see tab. 1. The wall of double forward facing step is heated at temperature of 310 K but the straight wall of pipe is unheated. Five different of volume concentration Hybrid Al<sub>2</sub>O<sub>3</sub>-Cu-water nanofluid varied for 0.1, 0.33, 0.75, 1, and 2. The series of Reynolds number different from 10000-40000 and computed based on inlet diameter,  $H$ , of the pipe.

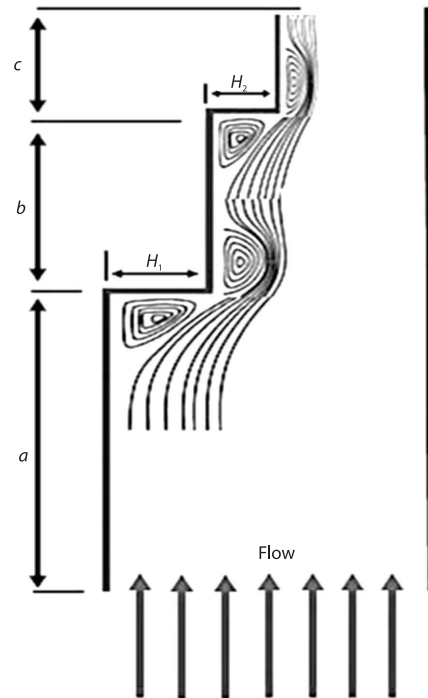


Figure 1. Diagram of current model

Table 1. Cases and dimension of geometry

Cases	$H$ (cm)	$H_1$ [cm]	$H_2$ [cm]	$a$ [cm]	$b$ [cm]	$c$ [cm]
1	5	1	1	80	40	20
2	5	2	1	80	40	20
3	5	1	2	80	40	20

Table 2. Physical properties of water and nanoparticles [51]

Physical properties	Water	Cu	Al <sub>2</sub> O <sub>3</sub>
$c_p$ [Jkg <sup>-1</sup> K <sup>-1</sup> ]	4179	385	765
$\rho$ [kg <sup>-1</sup> m <sup>-3</sup> ]	997.1	8933	3970
$k$ [Wm <sup>-1</sup> K <sup>-1</sup> ]	0.613	400	40
$\beta$ [1/K]	$21 \cdot 10^{-5}$	$1.67 \cdot 10^{-5}$	$0.85 \cdot 10^{-5}$
$\delta$ [ $\Omega^{-1}$ m <sup>-1</sup> ]	0.05	$5.96 \cdot 10^7$	$1 \cdot 10^{-10}$

**Table 3. Thermophysical properties of hybrid nanofluid [52]**

$\varphi$ [%]	$k_{nf}$ [Wm <sup>-1</sup> K <sup>-1</sup> ]	$\mu_{nf}$ [kg m <sup>-1</sup> s <sup>-1</sup> ]
0.10	0.6199817	0.000972
0.33	0.6309797	0.001098
0.75	0.6490042	0.001386
1.00	0.6570083	0.001602
2.00	0.6849921	0.001935

### Hybrid nanofluids properties

In this study, the hybrid nanofluids are suggested by nanoparticles of Al<sub>2</sub>O<sub>3</sub>-Cu in water as a base liquid with assume single-phase, incompressible and Newtonian fluid. Table 2 [51] are showed the properties of water, Al and Cu while tab. 3 are presented the thermal conductivity and dynamic viscosity of hybrid nanofluids as using based on [52]. From eqs. (1) and (2) can be calculated the density and specific heat capacity of Al<sub>2</sub>O<sub>3</sub>-Cu-water Hybrid nanofluids [52]:

$$\rho_{nf} = \varphi_{Cu}\rho_{Cu} + \varphi_{Al_2O_3}\rho_{Al_2O_3} + (1 - \varphi)\rho_f \quad (1)$$

$$(\rho c_p)_{nf} = \varphi_{Cu}(\rho c_p)_{Cu} + \varphi_{Al_2O_3}(\rho c_p)_{Al_2O_3} \quad (2)$$

where  $\varphi$  is the total of volume concentrations of both Al and Cu nanoparticles and is computed:

$$\varphi = \varphi_{Cu} + \varphi_{Al_2O_3} \quad (3)$$

where  $(\rho c_p)_f$  and  $(\rho c_p)_{np}$  represent the heat capacities of the base fluid and nanoparticles, respectively.

The effective thermal conductivity of solid-liquid mixtures was computed by [53, 54]:

$$k_{eff} = k_f \left[ \frac{k_p + 2k_f - 2\phi(k_f - k_p)}{k_p + 2k_f + \phi(k_f - k_p)} \right] \quad (4)$$

While correlation of viscosity was identified by [55]:

$$\mu_{eff} = \frac{\mu_f}{(1 - \phi)^{2.5}} \quad (5)$$

This correlation is employed for low volume fraction ( $\phi < 0.05$ ).

### Mathematical formulation

The set equations of continuity, momentum and energy can be presented:

$$\frac{\partial U_i}{\partial x_i} = 0 \quad (6)$$

$$\frac{\partial(U_i U_j)}{\partial x_j} = -\frac{\partial p}{\partial x_i} + \frac{\partial}{\partial x_j} \left( \mu \frac{\partial U_i}{\partial x_j} - \overline{\rho u_i u_j} \right) \quad (7)$$

$$\frac{\partial(U_i T_j)}{\partial x_j} = -\frac{\partial}{\partial x_i} \left( \frac{\mu}{Pr} \frac{\partial T_i}{\partial x_j} - \overline{\rho u_i t_j} \right) \quad (8)$$

The Reynolds stresses and heat fluxes are, respectively:

$$\overline{\rho u_i u_j} = -\mu_t \left( \frac{\partial U_i}{\partial x_j} + \frac{\partial U_j}{\partial x_i} \right) + \frac{2}{3} \delta_{ij} k \quad (9)$$

$$\overline{\rho u_i t_j} = -\frac{\mu_t \partial T_i}{\sigma_\theta \partial x_j} \quad (10)$$

The equations of standard  $k$ - $\varepsilon$  model can be written:

$$\frac{\partial \rho k U_i}{\partial x_j} = -\frac{\partial}{\partial x_j} \left[ \left( \mu + \frac{\mu_t}{\sigma_k} \right) \frac{\partial k}{\partial x_j} \right] + \rho (G_b - \varepsilon) \quad (11)$$

$$\frac{\partial \rho \varepsilon U_i}{\partial x_j} = -\frac{\partial}{\partial x_j} \left[ \left( \mu + \frac{\mu_t}{\sigma_k} \right) \frac{\partial \varepsilon}{\partial x_j} \right] + \rho \frac{\varepsilon}{k} (C_{1\varepsilon} G_b - C_{2\varepsilon} \varepsilon) \quad (12)$$

$$G_b = \mu_t \left( \frac{\partial u_i}{\partial x_j} + \frac{\partial u_j}{\partial x_i} \right) \frac{\partial u_i}{\partial x_j} \quad (13)$$

$$\mu_t = \rho C_\mu \frac{k^2}{\varepsilon} \quad (14)$$

The standard constants of model:

$$C_{1\varepsilon} = 1.44, C_{2\varepsilon} = 1.92, C_{3\varepsilon} = 0.09, \sigma_k = 1.0, \sigma_\varepsilon = 1.3, \text{ and } Pr = 7.01$$

In this study, 2<sup>nd</sup> order pattern was applied to achieve maximum numerical accuracy. The remaining amount was calculated and arranged for each repetition and the convergence measure was less than 10<sup>-8</sup> for the momentum and energy, and 10<sup>-6</sup> for the continuity equation.

### Solution procedure

Conservation equations are solved based on finite volume method for 2-D turbulent flow range and an incompressible with assume density of fluid is constant. In this simulation, ANSYS 14 ICEM software was adopted to construct the configuration while the heat transfer and flow equations were solved by ANSYS-FLUENT 14. For finding the accurate mesh, the ICEM tools for dealing with complex geometry were employed to create meshing process as shown in fig. 2. Standard  $k$ - $\varepsilon$  model was used to investigate the turbulent of hybrid Al<sub>2</sub>O<sub>3</sub>-Cu-water nanofluid and heat transfer over vertical DFFS. Case 1 was considered for test grid independent with pure water at Reynolds number of 30000.

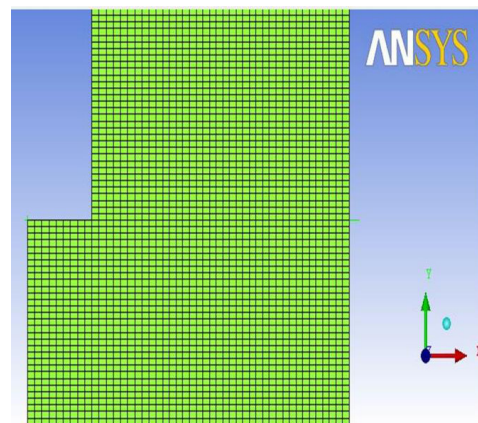
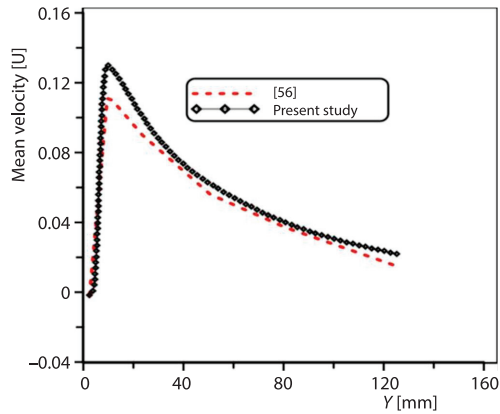


Figure 2. Structure of mesh



**Figure 3.** Comparison between the current results and previous data [57]

showed that the comparison between the current results and previous data of [56] where similar trend and great agreement were noticed for velocity distribution.

### Mesh-independent study and code validation

In order to get a mesh-independent, refinement the mesh size was done for stepwise and comparing the findings till the change is very small. Using pure water at Reynolds number of 30000 and Case 1 for mesh dimensions 9099, 37397, and 67117 were verified. The changes in Nusselt numbers found between the second and third meshes were less than 1%. Hence, a mesh size of 37397 was selected in this investigation. In order to verify the present model, investigate achieved by Abu-Mulaweh [56] was considered for effect of step heights on turbulent fluid-flow over a FFS. Figure 3

### Results and discussion

Influences of Reynolds number on local surface heat transfer factor for hybrid  $\text{Al}_2\text{O}_3$ -Cu-water nanofluid of 2% and Cases 1-3 are presented in figs. 4-6, respectively. The findings displayed that rises in local surface heat transfer factor with increased of Reynolds number and this is because greater velocity rises turbulence, which in turn delivers a more efficient radial transport/mixing of heat and gradually increments observed after 1<sup>st</sup> and 2<sup>nd</sup> steps for all cases and the highest heat transfer coefficient was seen at  $\text{Re} = 40000$  among the others. Moreover, fig. 7 shows the average heat transfer coefficient with Reynolds number for all cases and found that the highest average heat transfer coefficient was happens at Case 2 compared with Cases 1 and 3.

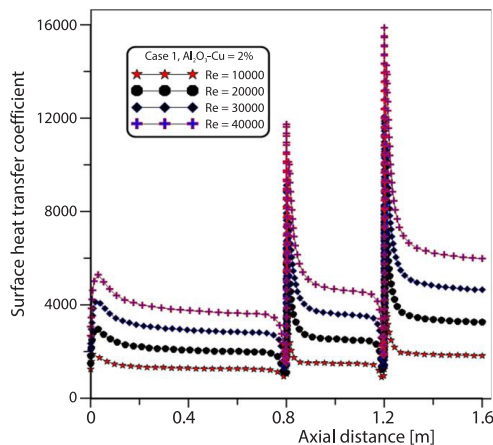


**Figure 4.** Profile of local surface heat transfer coefficient for hybrid  $\text{Al}_2\text{O}_3$ -Cu-water nanofluid of 2% and different Reynolds number at Case 1

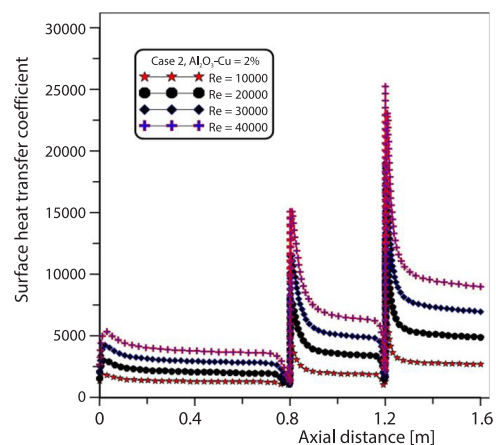


**Figure 5.** Profile of local surface heat transfer coefficient for hybrid  $\text{Al}_2\text{O}_3$ -Cu-water nanofluid of 2% and different Reynolds number at Case 2

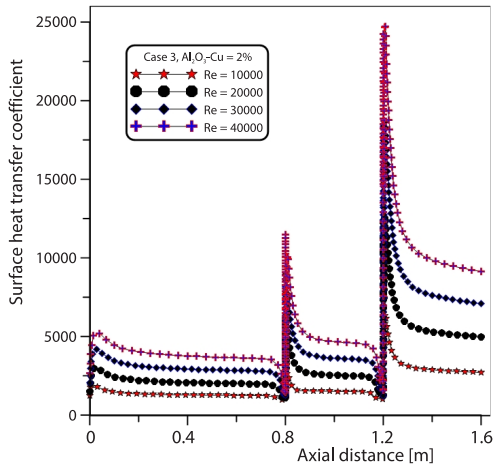


Figure 6. Profile of local surface heat transfer coefficient for hybrid Al<sub>2</sub>O<sub>3</sub>-Cu-water nanofluid of 2% and different Reynolds number at Case 3

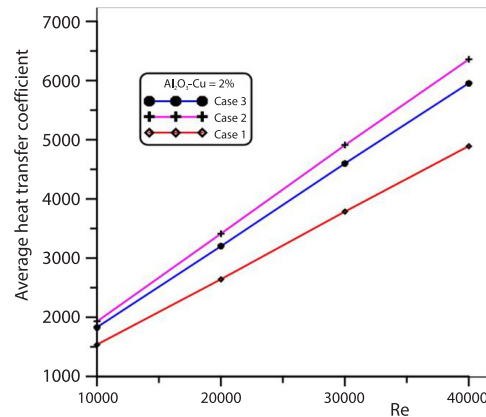


Figure 7. Average of heat transfer coefficient with different Reynolds number for Cases 1-3

Figures 8-10 are illustrated that distributions of local heat transfer coefficient for different volume fraction of hybrid Al<sub>2</sub>O<sub>3</sub>-Cu-water nanofluid at Cases 1-3, respectively. All cases has similar trends for the shape of surface heat transfer coefficients as increase of volume fraction of hybrid Al<sub>2</sub>O<sub>3</sub>-Cu-water nanofluid lead to rises in local heat transfer coefficients due to the convective heat transfer improvement of water based Al<sub>2</sub>O<sub>3</sub>-Cu hybrid nanofluids can be qualified to the actual thermal conductivity enhancement of water based Al<sub>2</sub>O<sub>3</sub>-Cu hybrid nanofluids because the heat transfer factor,  $h$ , is relational to thermal conductivity,  $k$ , and highest surface heat transfer coefficient found with 2% volume fraction of hybrid Al<sub>2</sub>O<sub>3</sub>-Cu-water nanofluid in compared with others. Influences of step height on surface heat transfer coefficients for Reynolds number of 40000 and 2% hybrid Al<sub>2</sub>O<sub>3</sub>-Cu-water nanofluid are demonstrated in fig. 11. Local heat transfer coefficient was highest at 1<sup>st</sup> step-Case 2 while was maximum at 2<sup>nd</sup> step-Case 3.

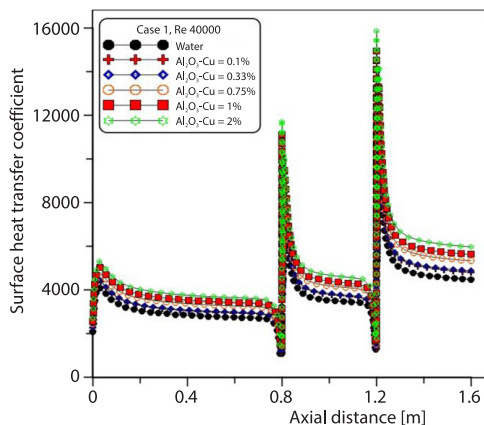


Figure 8. Variation of surface heat transfer coefficient for different volume fraction of hybrid Al<sub>2</sub>O<sub>3</sub>-Cu-water nanofluid at Case 1

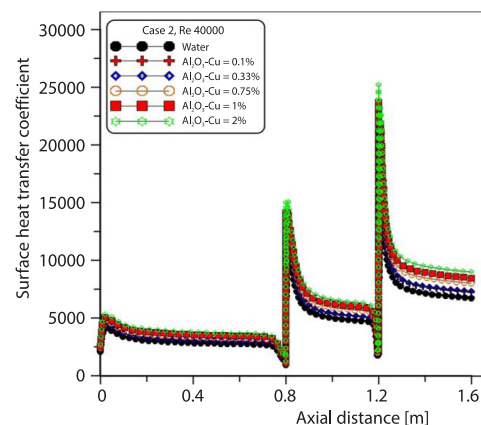


Figure 9. Variation of surface heat transfer coefficient for different volume fraction of hybrid Al<sub>2</sub>O<sub>3</sub>-Cu-water nanofluid at Case 2

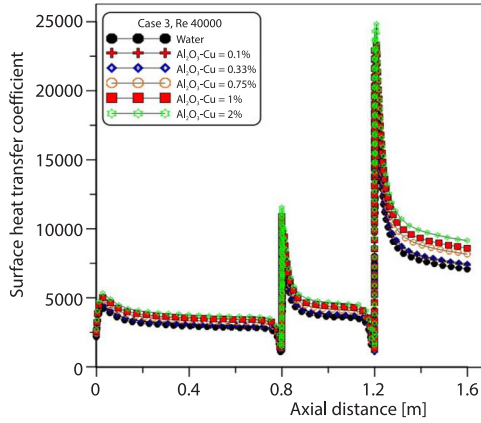


Figure 10. Variation of surface heat transfer coefficient for different volume fraction of hybrid Al<sub>2</sub>O<sub>3</sub>-Cu-water nanofluid at Case 3

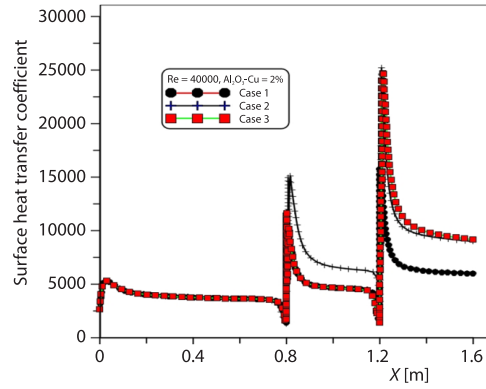


Figure 11. Effects of step height on surface heat transfer coefficients for Reynolds number of 40000 and 2% hybrid Al<sub>2</sub>O<sub>3</sub>-Cu-water nanofluid

The profile of local skin friction coefficient with different Reynolds number and 2% volume fraction of hybrid Al<sub>2</sub>O<sub>3</sub>-Cu-water nanofluid for Cases 1-3 are presented in figs. 12-14, respectively. Generally, reduction in local skin friction coefficient seen with increase of Reynolds number and gradually rises showed after 1<sup>st</sup> and 2<sup>nd</sup> steps for all cases and the lowest skin friction coefficient was seen at Reynolds number of 40000 among the others. Figure 13 shows that the effects of step heights on distributions of skin friction coefficient for Reynolds number of 40000 and 2% volume fraction of hybrid Al<sub>2</sub>O<sub>3</sub>-Cu-water nanofluid. The results indicated that maximum local skin friction coefficient was at 1<sup>st</sup> step-Case 2 but was bigger at 2<sup>nd</sup> step-Case 3.

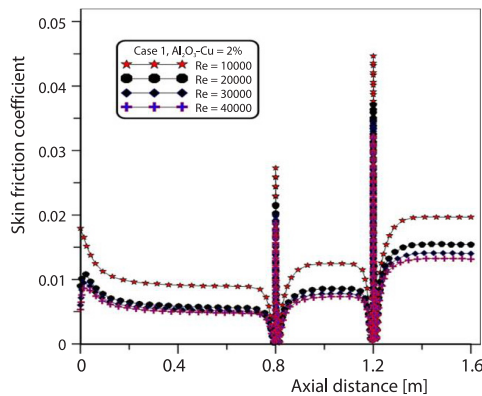


Figure 12. Profile of local skin friction coefficient with different Reynolds number and 2% volume fraction of hybrid Al<sub>2</sub>O<sub>3</sub>-Cu-water nanofluid for Case 1

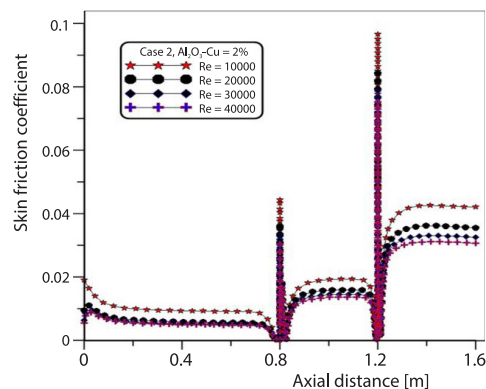
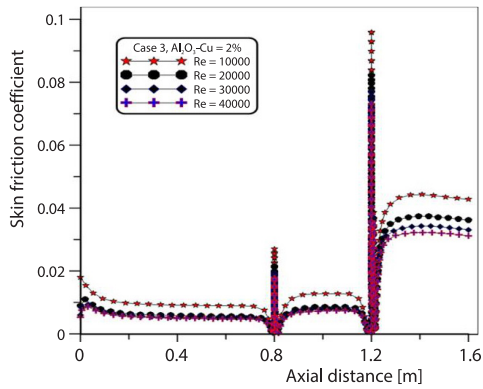
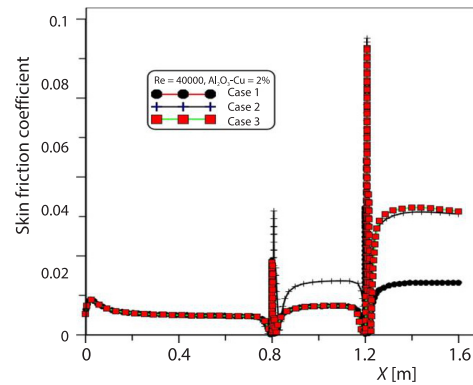


Figure 13. Profile of local skin friction coefficient with different Reynolds number and 2% volume fraction of hybrid Al<sub>2</sub>O<sub>3</sub>-Cu-water nanofluid for Case 2

Figure 15 shows that the effects of step heights on distributions of skin friction coefficient for Reynolds number of 40000 and 2% volume fraction of hybrid Al<sub>2</sub>O<sub>3</sub>-Cu-water nanofluid. The results indicated that maximum local skin friction coefficient was at 1<sup>st</sup> step-Case 2 but was bigger at 2<sup>nd</sup> step-Case 3. Counter of velocities at 1<sup>st</sup> and 2<sup>nd</sup> steps for Case 1



**Figure 14. Profile of local skin friction coefficient with different Reynolds number and 2% volume fraction of hybrid Al<sub>2</sub>O<sub>3</sub>-Cu-water nanofluid for Case 3**



**Figure 15. Effect of step heights on distributions of skin friction coefficient for Reynolds number of 40000 and 2% volume fraction of hybrid Al<sub>2</sub>O<sub>3</sub>-Cu-water nanofluid**

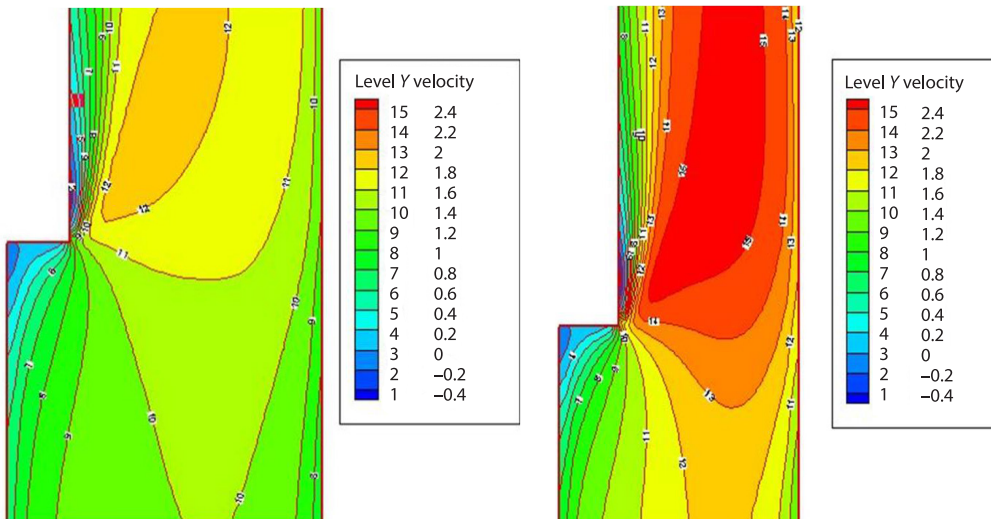


**Figure 16. Counter of velocities at 1<sup>st</sup> and 2<sup>nd</sup> steps for Case 1 and Reynolds number of 40000**

and Reynolds number of 40000 are displayed in the fig. 16. Two re-circulation zones have been seen before and after each step as illustrated the enhancement in heat transfer rate. The turbulent flux of turbulent kinetic energy displays in fig. 17 for Case 1 and different Reynolds number at 2% volume fraction of hybrid Al<sub>2</sub>O<sub>3</sub>-Cu-water nanofluid. The results found that enlargements in turbulence kinetic energy with increased Reynolds number and that is clearly seen after the 1<sup>st</sup> and 2<sup>nd</sup> steps. The biggest turbulent kinetic energy is detected after the 2<sup>nd</sup> step at Reynolds number 40000 which delivered demonstration for obtain thermal performance at second step for all cases.

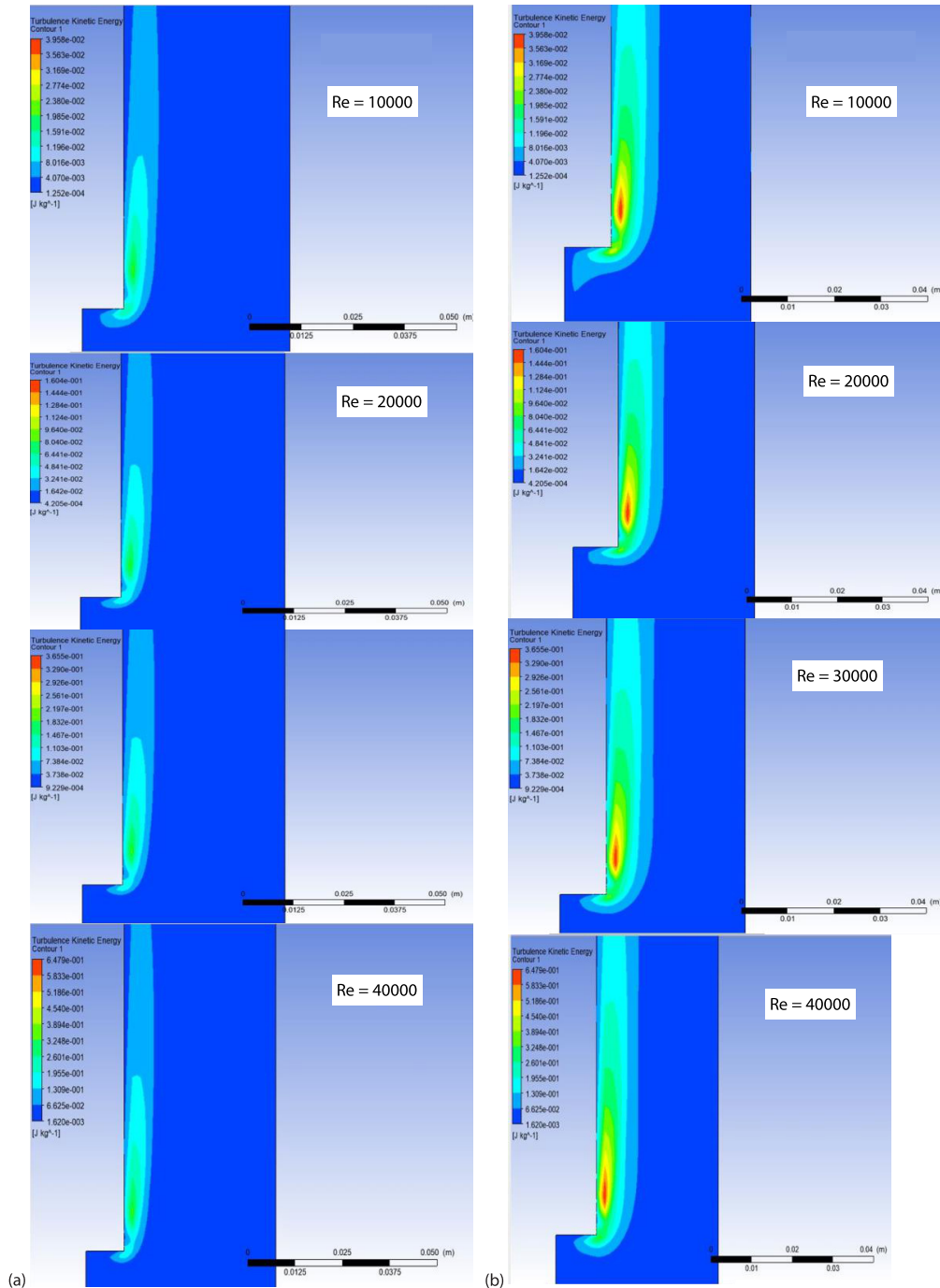


Figure 17. Counters of turbulence kinetic energy for Case 1 and Reynolds number of 40000; (a) 1<sup>st</sup> step and (b) 2<sup>nd</sup> step

## Conclusions

The recent research examine the effects of volume fraction of hybrid Al<sub>2</sub>O<sub>3</sub>-Cu-water nanofluid, Reynolds number, and step heights on heat transfer and flow characteristic. From the obtained results, the conclusion can be written as follows.

- Generally, increases of Reynolds number lead to rises in local surface heat transfer coefficient and usually augmentations seen especially after 1<sup>st</sup> and 2<sup>nd</sup> steps.
- The results clarified that highest heat transfer coefficient was found at Reynolds number of 40000 among the others.
- Maximum surface heat transfer coefficient found with 2% volume fraction of hybrid Al<sub>2</sub>O<sub>3</sub>-Cu-water nanofluid in compared with others.
- Influences of increases high of steps on surface heat transfer coefficients were described and was greater at 1<sup>st</sup> step-Case 2 while was greater at 2<sup>nd</sup> step-Case 3.
- Highest average heat transfer coefficient found occurs at Case 2 compared with Cases 1 and 3.
- Drop in local skin friction coefficient seen with rise in Reynolds number and the lowest skin friction coefficient was noticed at Reynolds number of 40000 among the others.
- Results showed that local skin friction coefficient was bigger at 1<sup>st</sup> step-Case 2 and at 2<sup>nd</sup> step-Case 3.

The effect of different kinds of hybrids nanofluid and base fluid on the thermal performance of DFF channels can be adopted for future work.

## Nomenclature

$a$  – length of bottom wall before the first step, [m]  
 $b$  – length of bottom wall after the first step, [m]  
 $c$  – length of bottom wall after the second step, [m]  
 $C_{1\epsilon}, C_{2\epsilon}, C_{3\epsilon}, \sigma_k, \sigma_\epsilon$  – model constants, [–]  
 $c_p$  – specific heat, [Jkg<sup>-1</sup>K<sup>-1</sup>]  
 $H$  – width of channel at entrance, [m]  
 $H_1$  – step height of first step, [m]  
 $H_2$  – step height of second step, [m]  
 $L$  – total length of channel, [m]  
 $k$  – turbulent energy, [m<sup>2</sup>s<sup>-2</sup>]  
 $Nu$  – Nusselt number, [–]  
 $p$  – pressure, [Pa]

$Pr$  – Prandtl number, [–]  
 $Re$  – Reynolds number, [–]  
 $T$  – temperature, [K]  
 $u, v$  – axial velocity, [ms<sup>-1</sup>]  
 $x, y$  – Cartesian co-ordinates, [m]

### Greek symbols

$\epsilon$  – turbulent energy dissipation, [m<sup>2</sup>s<sup>-3</sup>]  
 $\mu$  – dynamic viscosity, [kgm<sup>-1</sup>s<sup>-1</sup>]  
 $\mu_t$  – turbulent viscosity, [kgm<sup>-1</sup>s<sup>-1</sup>]  
 $\rho$  – water density, [kgm<sup>-3</sup>]

## References

- [1] Scheit, C., et al., Direct Numerical Simulation of Flow over a Forward-Facing Step – Flow Structure and Aeroacoustic Source Regions, *International Journal of Heat and Fluid-Flow*, 43 (2013), Oct., pp. 184-193
- [2] Alibek, I., Yeldos, Z., Investigation of Geometry Effect on Heat and Mass Transfer in Buoyancy Assisting with the Vertical Backward and Forward Facing Steps, *International Journal of Non-linear Sciences and Numerical Simulation*, 20 (2019), 3-4, pp. 407-431
- [3] Togun, H., et al., A., CFD Simulation of Heat Transfer and Turbulent Fluid-flow over a Double Forward-Facing Step, *Mathematical Problems in Engineering*, 2013 (2013), ID895374
- [4] Biswas, G., et al., Backward-Facing Step Flows for Various Expansion Ratios at Low and Moderate Reynolds Number, *Journal of Fluids Engineering*, 126 (2004), 3, pp. 362-374
- [5] Armaly, B. F., et al., Experimental and Theoretical Investigation of Backward-Facing Step Flow, *Journal of Fluid Mechanics*, 127 (1983), Feb., pp. 473-496
- [6] Oztop, H. F., et al., Analysis of Turbulent Flow and Heat Transfer over a Double Forward Facing Step with Obstacles, *International Communications in Heat and Mass Transfer*, 39 (2012), 9, pp. 1395-1403
- [7] Hilo, A. K., et al., Effect of Corrugated Wall Combined with Backward-Facing Step Channel on Fluid-Flow and Heat Transfer, *Energy*, 190 (2020), 116294

- [8] SriHarsha, V., et al., Influence of Rib Height on the Local Heat Transfer Distribution and Pressure Drop in a Square Channel with 90° continuous and 60° V-Broken Ribs, *Applied Thermal Engineering*, 29 (2009), 11-12, pp. 2444-2459
- [9] Promvongse, P., Heat Transfer and Pressure Drop in a Channel with Multiple 60° V-Baffles, *International Communications in Heat and Mass Transfer*, 37 (2010), 7, pp. 835-840
- [10] Togun, H., et al., An Experimental Study of Turbulent Heat Transfer Separation External in an Annular Passage, *Proceedings, International Conference on Applications and Design in Mechanical Engineering (ICADME 2009)*, Universiti Malaysia Perlis, Perlis, Malaysia, 2009
- [11] Sherry, M., et al., An Experimental Investigation of the Re-Circulation Zone Formed Downstream of a Forward Facing Step, *Journal Wind Engng Ind. Aerodyn.*, 98 (2010), 12, pp. 888-894
- [12] Togun, H., et al., A Review of Experimental Study of Turbulent Heat Transfer in Separated Flow, *Australian Journal of Basic and Applied Sciences*, 5 (2011), 10, pp. 489-505
- [13] Lanzerstorfer, D., Kuhlmann, H. C., The 3-D Instability of the Flow over a Forward-Facing Step, *Journal Fluid Mech.*, 695 (2012), Feb., pp. 390-404
- [14] Togun, H., et al., An Experimental Study of Heat Transfer to Turbulent Separation Fluid-Flow in an Annular Passage, *International Journal of Heat and Mass Transfer*, 54 (2011), 4, pp. 766-773
- [15] Gupta, A., et al., Local Heat Transfer Distribution in a Square Channel with 90° Continuous, 90° Saw Tooth Profiled and 60° Broken Ribs, *Experimental Thermal and Fluid Science*, 32 (2008), 4, pp. 997-1010
- [16] Oon, C. S., et al., Computational Simulation of Heat Transfer to Separation Fluid-Flow in an Annular Passage, *International Communications in Heat and Mass Transfer*, 46 (2013), Aug., pp. 92-96
- [17] Hussein, T., et al., Numerical Study of Turbulent Heat Transfer in Separated Flow: Review, *International Review of Mechanical Engineering (IREME)*, 7 (2013), 2, pp. 337-349
- [18] Sherry, M., et al., An Experimental Investigation of the Re-Circulation Zone Formed Downstream of a Forward Facing Step, *Journal Wind Engng Ind. Aerodyn.*, 98 (2010), 12, pp. 888-894
- [19] Togun, H., et al., Heat Transfer to Laminar Flow over a Double Backward-Facing Step, *World Academy of Science, Engineering and Technology, International Journal of Mechanical Science and Engineering*, 7 (2013), 8, pp. 961-966
- [20] Hattori, H., Nagano, Y., Investigation of Turbulent Boundary-Layer over Forward-Facing Step Via Direct Numerical Simulation, *Intl J. Heat Fluid-Flow*, 31 (2010), 3, pp. 284-294
- [21] Togun, H., et al., Numerical Study of Turbulent Heat Transfer in Annular Pipe with Sudden Contraction, *Applied Mechanics and Materials*, 465-466 (2013), Dec., pp. 461-466
- [22] Hajji, H., et al., Heat Transfer and Flow Structure through a Backward-and Forward-Facing Step Micro-Channels Equipped with Obstacles, *Thermal Science*, 25 (2021), 4A, pp. 2483-2492
- [23] Selimefendigil, F., Oztop, H. F., Numerical Study of Forced Convection of Nanofluid-Flow over a Backward Facing Step with a Corrugated Bottom Wall in the Presence of Different Shaped Obstacles, *Heat Transfer Engineering*, 37 (2016), 15, pp. 1280-1292
- [24] Chamkha, A. J., Selimefendigil, F., Forced Convection of Pulsating Nanofluid-Flow over a Backward Facing Step with Various Particle Shapes, *Energies*, 11 (2018), 11, pp. 1-19
- [25] Selimefendigil, F., Oztop, H. F., The MHD Pulsating Forced Convection of Nanofluid over Parallel Plates with Blocks in a Channel, *International Journal of Mechanical Sciences*, 157 (2019), July, pp. 726-740
- [26] Hussein, T., et al., Numerical Simulation of Heat Transfer and Separation Al<sub>2</sub>O<sub>3</sub>/Nanofluid-Flow in Concentric Annular Pipe, *International Communications in Heat and Mass Transfer*, 71 (2016), Feb., pp. 108-117
- [27] Tuqa, A., et al., Turbulent Heat Transfer and Nanofluid-Flow in an Annular Cylinder with Sudden Reduction, *Journal of Thermal Analysis and Calorimetry*, 141 (2020), Mar., pp. 373-385
- [28] Abdulrazzaq, T., et al., Effect of Flow Separation of TiO<sub>2</sub> Nanofluid on Heat Transfer in the Annular Space of Two Concentric Cylinders, *Thermal Science*, 24 (2020), 2A, pp. 1007-1018
- [29] Hussein, T., Laminar CuO-Water Nanofluid-Flow and Heat Transfer in a Backward-Facing Step with and without Obstacle, *Applied Nanoscience*, 6 (2016), 3, pp.371-378
- [30] Tuqa, A., et al., Heat Transfer Improvement in a Double Backward-Facing Expanding Channel Using Different Working Fluids, *Symmetry*, 12 (2020), 7, pp. 1-23
- [31] Hilo, A. K., et al., Heat Transfer and Thermal Conductivity Enhancement using Graphene Nanofluid: A Review, *Journal of Advanced Research in Fluid Mechanics and Thermal Sciences*, 55 (2019), 1, pp. 74-87
- [32] Hussein, T., et al., Turbulent Heat Transfer to Separation Nanofluid-Flow in Annular Concentric Pipe, *International Journal of Thermal Sciences*, 117 (2017), July, pp.14-25
- [33] Salman, S, Abd Rahim, A. T., Numerical Study on the Turbulent Mixed Convection Heat Transfer over 2-D Microscale Backward Facing Step, *CFD Letters*, 11 (2019), 10, pp. 31-45

- [34] Togun, H., Experimental and Numerical Study of Heat Transfer to Nanofluid-Flow in Sudden Enlargement of Annular Concentric Pipe, Ph. D. thesis, University of Malay, Kuala Lumpur, Malaysia, 2015
- [35] Kherbeet, A. S., et al., Combined Convection Nanofluid-Flow and Heat Transfer over Microscale Forward-Facing Step, *Int. J. Nanoparticle*, 6 (2013), 4, pp. 350-365
- [36] Kherbeet, A. S., et al., Experimental and Numerical Study of Nanofluid-Flow and Heat Transfer over Microscale Forward-Facing Step, *International Communications in Heat and Mass Transfer*, 57 (2014), Oct., pp. 319-329
- [37] Hussein, T., et al., Numerical Simulation of Laminar to Turbulent Nanofluid-Flow and Heat Transfer over a Backward-Facing Step, *Applied Mathematics and Computation*, 239 (2014), July, pp. 153-170
- [38] Togun, H., et al., Thermal Performance of Nanofluid in Ducts with Double Forward-Facing Steps, *Journal of the Taiwan Institute of Chemical Engineers*, 47 (2015), Feb., pp. 28-42
- [39] Safaei, M. R., et al., Investigation of Heat Transfer Enhancement in a Forward-Facing Contracting Channel Using FMWCNT Nanofluids, *Numerical Heat Transfer – Part A: Applications*, 66 (2014), 12, pp. 1321-1340
- [40] Selimefendigil, F., Oztop, H. F., Laminar Convective Nanofluid-Flow over a Backward-Facing Step with an Elastic Bottom Wall, *Journal of Thermal Science and Engineering Applications*, 10 (2018), 041003
- [41] Ahmed, S. M., et al., Toward Improved Heat Dissipation of the Turbulent Regime over Backward-Facing Step for the Alumina-Water Nanofluids – An Experimental Approach, *Thermal Science*, 23 (2019), 3, pp. 1779-1789
- [42] Turcu, R., et al., New Polypyrrole-Multiwall Carbon Nanotubes Hybrid Materials, *Journal Optoelectron. Adv. Mater*, 8 (2006), 2, pp. 643-647
- [43] Jana, S., et al., Enhancement of Fluid Thermal Conductivity by the Addition of Single and Hybrid Nanoadditives, *Thermochim. Acta*, 462 (2007), 1-2, pp. 45-55
- [44] Saha, G., Finite Element Simulation of Magneto Convection Inside a Sinusoidal Corrugated, Journal Pre-proof Journal Pre-proof 47 Enclosure with Discrete is Flux Heating from Below, *Int. Commun. Heat Mass Transfer*, 37 (2010), 4, pp. 393-400
- [45] Hussain, S. H., et al., Studying the Effects of a Longitudinal Magnetic Field and Discrete Isoflux Heat Source Size on Natural-Convection Inside a Tilted Sinusoidal Corrugated Enclosure, *Comput. Math. with Appl.*, 64 (2012), 4, pp. 476-488
- [46] Takabi, B., Salehi, S., Augmentation of the Heat Transfer Performance of a Sinusoidal Corrugated Enclosure by Employing Hybrid Nanofluid, *Adv. Mech. Eng.*, 2014 (2014), ID147059
- [47] Mehrez, Z., El Cafsi, A., Forced Convection Magnetohydrodynamic Al<sub>2</sub>O<sub>3</sub>-Cu/Water Hybrid Nanofluid-Flow over a Backward-Facing Step, *Journal Therm. Anal. Calorim.*, 135 (2018), July, pp. 1417-1427
- [48] Hilo, A. K., et al., Experimental Study of Nanofluids Flow and Heat Transfer over a Backward-Facing Step Channel, *Powder Technology*, 372 (2020), July, pp. 497-505
- [49] Salman, S., et al., Hybrid Nanofluid-Flow and Heat Transfer over Backward and Forward Steps: A Review, *Powder Technology*, 363 (2020), Mar., pp. 448-472
- [50] Abdulrazzaq, T., et al., Heat Transfer and Turbulent Fluid-flow over Vertical Double Forward-Facing Step, *International Journal of Aerospace and Mechanical Engineering*, 8 (2014), 2, pp. 368-372
- [51] Abu-Nada E., Application of Nanofluids for Heat Transfer Enhancement of Separated Flows Encountered in a Backward Facing Step, *Int. J. Heat Fluid-Flow*, 29 (2008), 1, pp. 242-249
- [52] Takabi, B., et al., Hybrid Water-Based Suspension of Al<sub>2</sub>O<sub>3</sub> and Cu Nanoparticles on Laminar Convection Effectiveness, *Journal Thermophys Heat Transf.*, 30 (2016), 3, pp. 523-532
- [53] Xuan, Y., Roetzel, W., Conceptions for Heat Transfer Correlation of Nanofluids, *International Journal of Heat and Mass Transfer*, 43 (2000), 19, pp. 3701-3707
- [54] Wang, H. L. B.-X., Peng, X. F., Research on the Heat-Conduction Enhancement for Liquid with Nanoparticle Suspensions, General Paper (G-1), *Proceedings*, International Symposium on Thermal Science and Engineering (TSE2002), Beijing, China, 2000
- [55] Brinkman, H. C., The Viscosity of Concentrated Suspensions and Solutions, *The Journal of Chemical Physics*, 20 (1952), 4, pp. 571-571
- [56] Abu-Mulaweh, H. I., Turbulent Mixed Convection Flow over a Forward Facing Step – The Effect of Step Heights, *International Journal of Thermal Sciences*, 44 (2015), 2, pp.155-162